

Lawrence Berkeley National Laboratory

Lawrence Berkeley National Laboratory

Title

Beam measurements on the H- source and Low Energy Beam Transport system for the Spallation Neutron Source

Permalink

<https://escholarship.org/uc/item/9dn871t9>

Authors

Thomae, R.
Gough, R.
Keller, R.
et al.

Publication Date

2001-09-01

**Beam measurements on the H⁻ Source and Low Energy Beam Transport
system for the Spallation Neutron Source***

R. Thomae, R. Gough, R. Keller, K.N. Leung, T. Schenkel, *Lawrence Berkeley National
Laboratory, Berkeley, CA, USA*

A. Aleksandrov, M. Stockli, R. Welton, *Oak Ridge National Laboratory, Oak Ridge, Oak
Ridge, TN, USA*

Abstract

The ion source and Low Energy Beam Transport section of the front-end systems presently being built by Berkeley Lab are required to provide 50 mA of H⁻ beam current at 6% duty factor (1 ms pulses at 60 Hz) with a normalized rms emittance of less than 0.20 mm-mrad. Experimental results, including emittance, chopping, and steering measurements, on the performance of the ion source and LEBT system operated at the demanded beam parameters will be discussed.

1. Introduction

Berkeley Lab is engaged in the construction of the front-end systems (FES) of the Spallation Neutron Source (SNS) presently being built at Oak Ridge National Laboratory [1,2]. Two subsystems of the front end are the ion source and the Low Energy Beam Transport (LEBT) section. The ion source, enabling SNS to achieve 1.44-MW average beam power, is supposed to provide 50 mA of H^- beam current at 6% duty factor (1 ms pulses at 60 Hz) with a normalized rms emittance of 0.20 mm mrad. The H^- beam is generated in a radio-frequency driven, magnetically filtered multicusp ion source. Extracted electrons are separated from the negative ion beam by a strong dipole magnet located in the outlet electrode and are then deposited on a dumping electrode inside the extraction gap. To compensate for the associated bending of the H^- beam, the source is tilted by a few degrees. The LEBT system, with a total length of only 10 cm, is all electrostatic to prevent variability of the space charge compensation and consists of two Einzel lenses, the second of which is also used for beam steering and chopping. The H^- beam is accelerated to 65 keV and matched into the 2.5 MeV RFQ. An overview of the achieved system performance is given elsewhere [3], and this paper predominantly discusses experimental results with ion source and LEBT that were obtained in preparation of RFQ beam tests.

2. Experimental setup

The FES integrated test stand consists of the ion source, the vacuum chamber with the all-electrostatic LEBT section, the tank for the beam diagnostics, and associated infrastructure. The ion source and LEBT system are shown schematically in fig. 1. The source is mounted inside a reentrant-cylinder to position it within the LEBT vacuum vessel. This arrangement provides good vacuum pumping speed near the extraction gap. The cylindrical source plasma chamber (10 cm long by 10-cm diameter) is made out of stainless steel with a back plate at one end and an outlet electrode at the other. The plasma is confined by the longitudinal line-cusp fields produced by 20 rows of water-cooled, samarium-cobalt magnets that surround the source chamber and by four additional rows of magnets on the back flange. The hydrogen plasma is sustained by up to 40 kW of pulsed 2 MHz RF power. The inductive RF power coupling to the plasma is accomplished via a 2 1/2-turn, porcelain-coated copper antenna. A pair of water-cooled permanent magnet rods placed near the outlet electrode creates a narrow region of transverse magnetic filter field (200 G peak strength) that divides the source chamber into the ("hot-plasma") main discharge region and the ("cold-plasma") H⁻ production region. A double-walled steel collar (15-mm diameter, 10-mm long) is mounted on the outlet electrode with minimized thermal conduction, facing the plasma side and holds 8 tiny cesium getter containers inside longitudinal grooves. Active cooling or heating - depending on the discharge duty factor - is made possible by adjusting a temperature-regulated airflow through the collar jacket. Cesium coverage of the collar surface lowers its work function, thereby increasing the H⁻ ion density in the cold-plasma region. The outlet electrode consists of a copper plate, a soft iron plate for magnetic field shaping, a number of permanent magnets in the so-called Halbach configuration [4] and a stainless

steel plate with the outlet aperture. Downstream of this aperture the magnets generate a transversely homogeneous dipole field of 1700 Gauss peak strength. The dipole field deflects the electrons to the plasma chamber or to the suppression (“dumping”) electrode, but slightly steers the H^- beam as well. Therefore the source is tilted at an angle of about 3° with respect to the beam axis to compensate the deflection.

The LEBT optical system consists essentially of four electrodes: The extractor, first lens, ground, and second lens, which are used to transport and match the extracted beam from the source to the entrance of the RFQ accelerator. The second lens electrode consists of four isolated segments which can be biased independently. This allows for beam steering and beam chopping. The beam then enters the diagnostic chamber via an entrance flange with an aperture of 13 mm. In the diagnostic chamber a magnetically shielded Faraday cup collects the beam. To determine the beam quality, two Allison-type emittance scanners are used [5]. The steering and chopping experiments have been carried out with the first RFQ module attached to the LEBT. The RFQ entrance flange, which also functions as the LEBT exit flange, has an aperture of 9 mm.

3. Experimental results

The RF-driven source is operated with an RF power of 25-40 kW and a continuous hydrogen gas flow of 20-30 sccm. Different plasma ignition schemes have been tested [6]. All measurements have been carried out with a collar temperature of 200 - 300 $^\circ\text{C}$, to ensure cesium coverage. The beam energy is 65 keV for all experiments. The lens potentials are typically -40 kV.

H⁻ pulse currents up to 50 mA have been extracted from the source and transported through the LEBT. In the following, beam measurements are described which have been performed with the extraction gap distance increased from 7.8 to 12.4 mm (measured from the surface of the electron suppression to the surface of the extraction electrode). This value was chosen to better match the beam at the reduced current of ~30 mA which was selected for first RFQ beam injection tests. In fig. 2 the shape of a 30 mA averaged current with a somewhat higher peak value shortly after ignition, 350 μ s pulse at a repetition frequency of 10 Hz is shown (trace 1). Trace 4 shows the RF gate and trace 3 shows the 1 kV-drop of the source potential during the pulse.

The horizontal (x-x') and vertical (y-y') emittance diagrams of the beam are shown in fig. 3a and b, measured 43 mm behind the exit plane of the second LEBT lens. For voltages of -42 kV for both lenses, the diagrams show convergent beams in both planes, with pronounced aberrations in the 10 % intensity level. The normalized rms-emittances were determined as: $\epsilon_h = 0.39$ mm mrad (horizontal) and $\epsilon_v = 0.34$ mm mrad (vertical) for these conditions. The Twiss parameters α and β are calculated from the distributions to be: $\alpha_h = -0.23$, $\alpha_v = -0.18$ and $\beta_h = 0.04$ mm/mrad, $\beta_v = 0.03$ mm/mrad. Obviously, these values are strongly influenced by LEBT aberrations. When the beam current is reduced by 30 % most of the aberrations are eliminated, and the distribution yields: $\epsilon_h = 0.15$ mm mrad, $\epsilon_v = 0.09$ mm mrad and $\alpha_h = 0.20$, $\alpha_v = 1.20$ and $\beta_h = 0.03$ mm/mrad, $\beta_v = 0.03$ mm/mrad. In fig. 4a and b, the Twiss parameters α and β are plotted for different lens voltages. The figures show that the beam diameter and envelope angle can be varied

over a wide range. Furthermore, it is evident that the beam is not symmetric, which is caused by stronger aberrations in the horizontal plane where the magnetic forces are acting in the extraction gap. The acceptance values of the RFQ have been determined by PARMTEQ simulations to: $\epsilon_{h} = \epsilon_{v} = 0.20$ mm mrad, $\epsilon_{h} = \epsilon_{v} = 1.5$ and $\epsilon_{h} = \epsilon_{v} = 0.06$ mm/mrad. For lens voltages of -42 kV for both lenses best matching into the RFQ is expected [7]. Transmission experiments with the first RFQ module verified these results [2].

First experimental results on the steering action of lens two are given in fig. 5. These experiments were carried out in combination with the RFQ attached to the LEBT and powered to full gradient. The measured H^{-} current as a function of the applied voltage difference between two pairs of segments is plotted. The transmission is highest when no steering voltage is applied and decreases to almost zero for $+3$ or -3 kV, an indication of good system alignment. This was also confirmed by emittance measurements.

In fig. 6 the transmitted current is shown when the beam chopping system is used in the LEBT. This system produces $0 - 3$ kV voltage pulses typically 300 ns in length with a rise and fall time of slightly less than 50 ns, which provides the necessary beam gaps in the pulse for beam extraction from the SNS accumulator ring. The chopping ratio is defined as the fraction of current transmitted while a chopping voltage is applied to two pairs of segments of lens 2. The figure shows that less than 1% of the beam intensity remains with ± 2 kV chopping voltage. The measured rise and fall time of the beam was determined to be of the order of 25 ns, faster than the high-voltage switching speed

because part of the beam is intercepted at less than the nominal chopping amplitude. Due to voltage breakdown occurring in the chopper circuitry, no experiments have yet been carried out at the design voltage of $\pm 3\text{kV}$.

4. Conclusion

The measurements presented demonstrate that the ion source and LEBT are capable of producing and transporting an intense H^- ion beam with the required quality for RFQ injection.

Acknowledgements

This work is supported by the Director, Office of Science, Office of Basic Energy Science, of the U.S. Department of Energy under Contract No. DE-AC03-76SF00098.

Many people are involved in the setup of the front-end systems. We would like to thank everybody for constant effort and support.

References

- [1] www.sns.gov

- [2] R. Keller et al., "Progress with the SNS Front-End Systems", Proceedings of PAC 2001, Paper MOPB005, Chicago (2001).

- [3] R. Keller et al., "Ion-source and LEBT Issues with the Front-End Systems for the Spallation Neutron Source", these proceedings, ICIS '01, Oakland (2001).

- [4] K. Halbach, Nucl. Instrum. Methods, 169, p. 1, (1980).

- [5] P. Allison, J. Sherman, and D. Holtkamp, IEEE Trans. Nucl. Sci., NS-30, p. 2204 (1983).

- [6] T. Schenkel et al., "Plasma Ignition Schemes for the SNS Radio-Frequency Driven H Source", these proceedings, ICIS '01, Oakland (2001).

- [7] R. Welton et al., "Simulations of the Ion Source Extraction and Low-Energy Beam Transport System for the Spallation Neutron Source Accelerator", these proceedings, ICIS '01, Oakland (2001).

Figure captures

Figure 1: Schematic of the ion source and Low Energy Beam Transport section. . The H⁻ beam is generated in a radio-frequency driven, magnetically-filtered multicusp ion source. Extracted electrons are separated from the negative ion beam by a strong dipole magnet located in the outlet electrode and are then deposited on a dumping electrode inside the extraction gap. To compensate for the associated bending of the H⁻ beam, the source is tilted by a few degrees with respect to the LEBT axis. Note that the actual filter and electron-dumping magnetic field are oriented orthogonally to the illustration plane. The shape of the beam envelope is exaggerated for emphasis.

Figure 2: Shape of a 30 mA averaged current, 350 μ s pulse at a repetition frequency of 10 Hz (trace 1). Trace 4 shows the RF gate and trace 3 shows the 1 kV-drop of the source potential during the pulse.

Figure 3: (a) The horizontal (x-x') and (b) vertical (y-y') emittance diagrams of a 30 mA beam, measured 43 mm behind the exit plane of the second LEBT lens. Both lens voltages are -42 kV. The normalized rms-emittances were determined as: $\epsilon_h = 0.39$ mm mrad (x-x') and $\epsilon_v = 0.34$ mm mrad (y-y'). The Twiss parameters α and β are calculated

from the distributions to be: $\epsilon_h = -0.23$, $\epsilon_v = -0.18$ and $\epsilon_h = 0.04$ mm/mrad, $\epsilon_v = 0.03$ mm/mrad.

Figure 4: The Twiss parameters ϵ_h and ϵ_v for different lens voltages. The beam current is 30 mA for all measurements. Results are plotted in (a) for the horizontal plane and in (b) for the vertical plane.

Figure 5: Steering action of lens 2. These experiments were carried out in combination with the RFQ attached to the LEBT and powered to full gradient. Shown is the measured H^- current as a function of the applied voltage difference between two pairs (AD and BC) of segments is plotted.

Figure 6: The transmitted current is shown when the beam chopping system is used in the LEBT. The chopping system produces 0 – 3 kV voltage pulses typically 300 ns in length with a rise and fall time of slightly less than 50 ns. The chopping ratio is defined as the fraction of current transmitted while a chopping voltage is applied to two pairs of segments of lens 2.

Figure 1

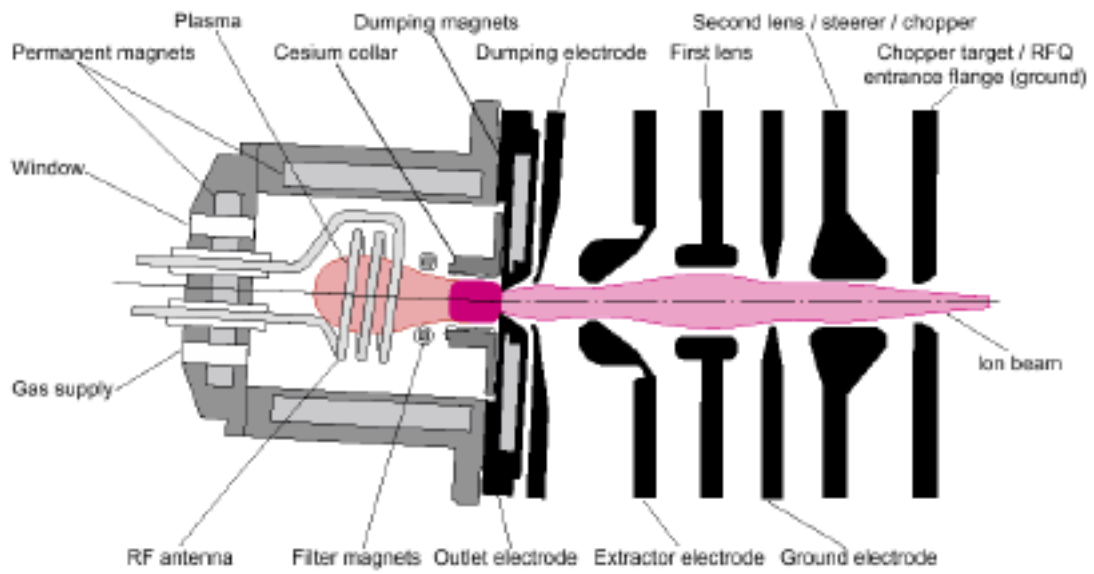


Figure 2

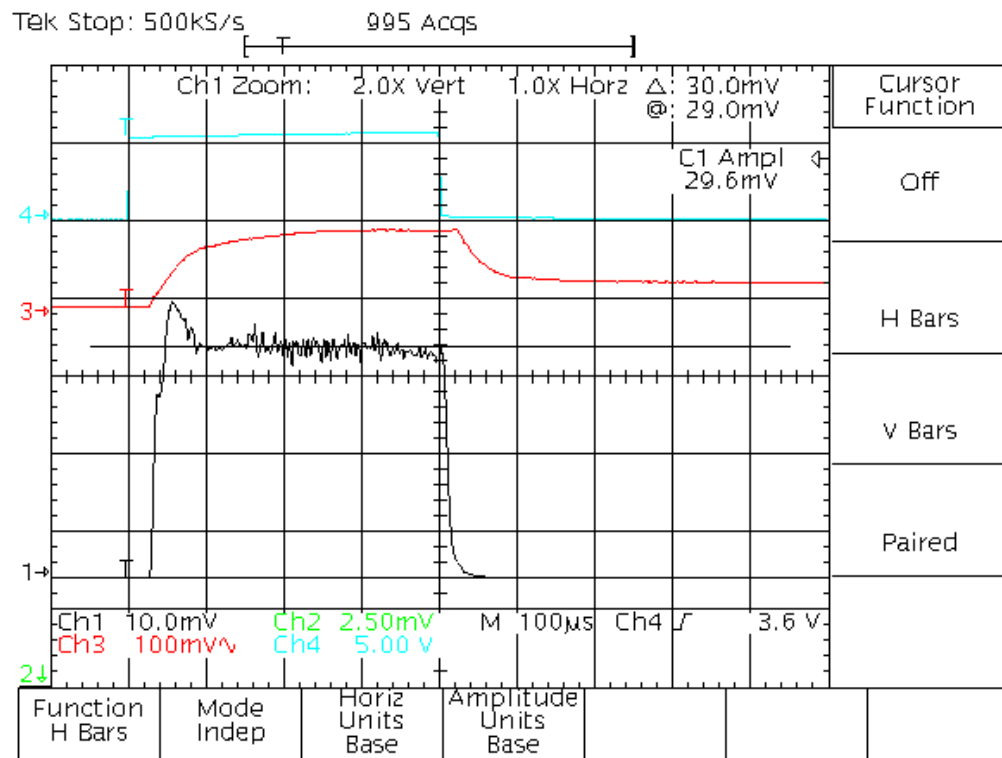


Figure 3a

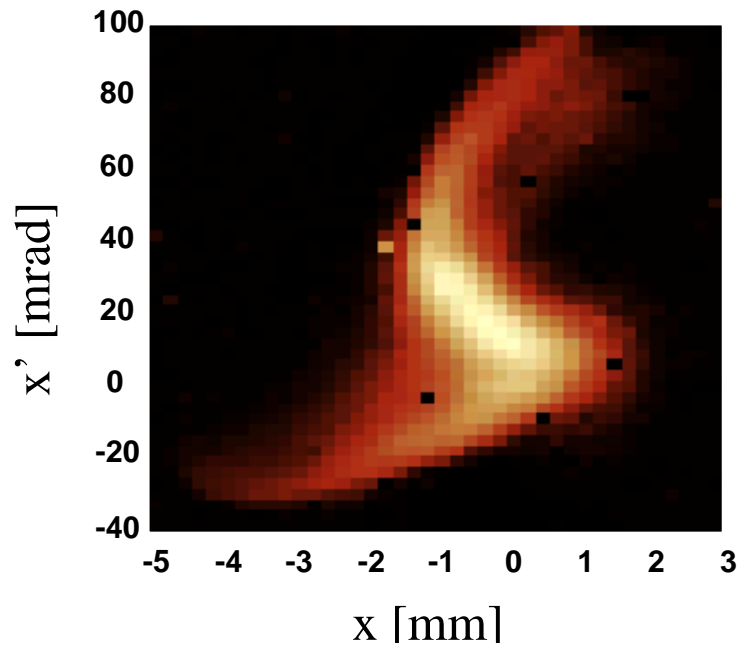


Figure 3b

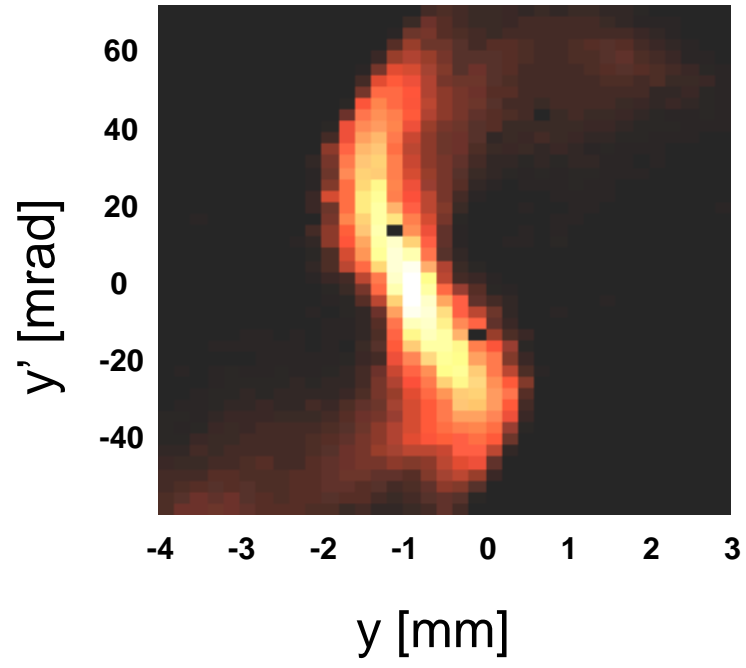


Figure 4a

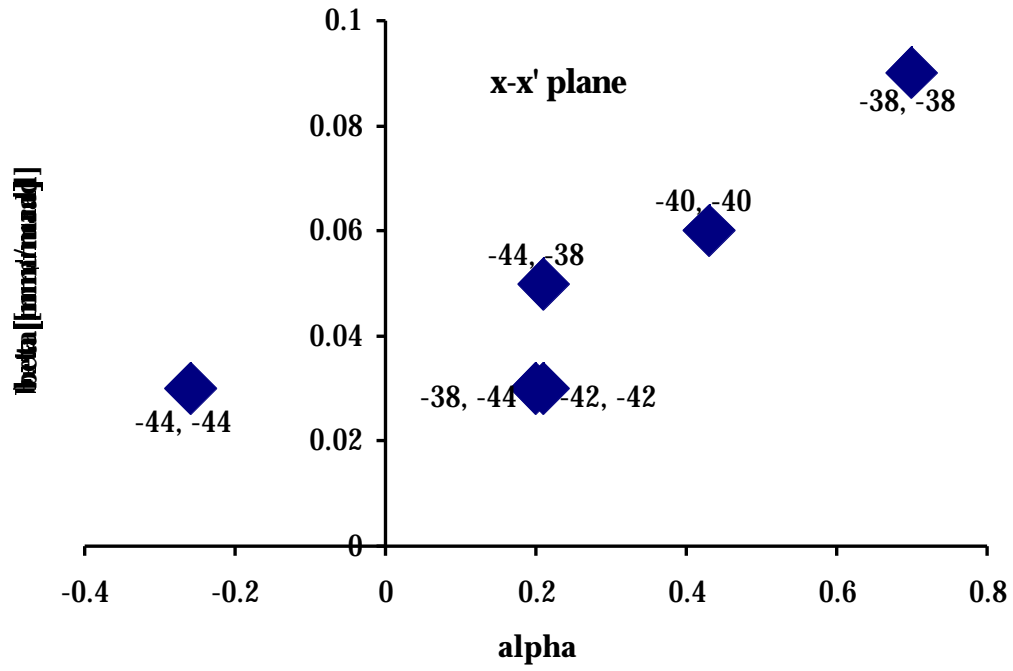


Figure 4b

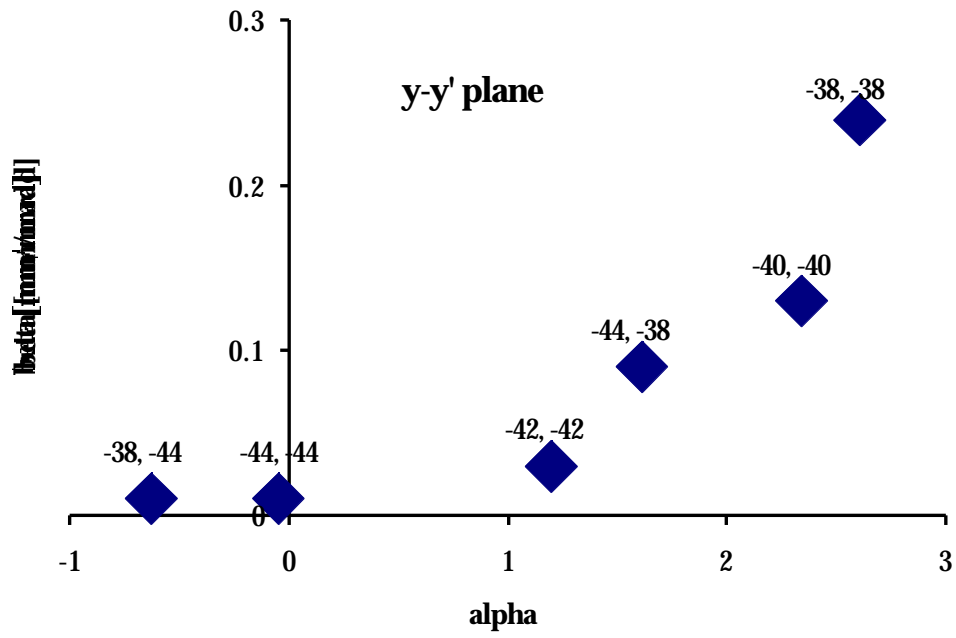


Figure 5

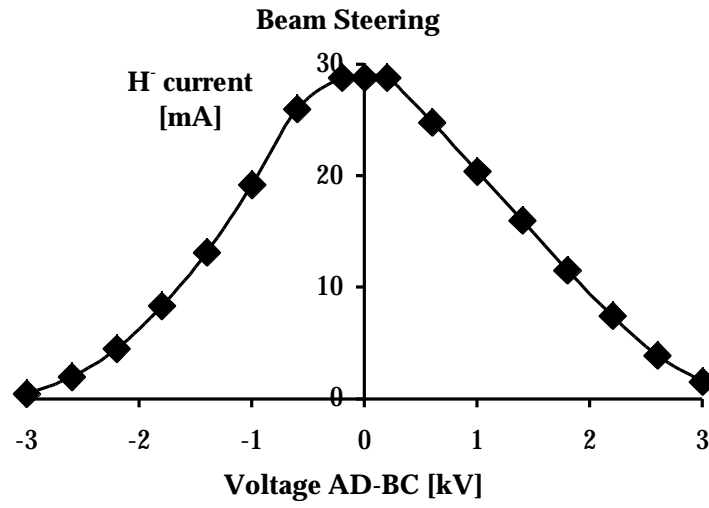


Figure 6

